To test this possibility further, we quantified the recruitment of these signaling proteins to local sites of integrin ligation. Skap2 recruitment to integrin-directed beads was impaired in *Sirpα*$^{\Delta/\Delta}$ cells; by contrast, Sirpα recruitment to engaged integrins was not significantly reduced in *Skap2*$^{-/-}$ BMMs (Fig. 7A). Indeed, in these cells, the Sirpα staining pattern showed small accumulations that were deficient in actin (Fig. 7A). As expected, Adap, which binds stoichiometrically to Skap2, was not recruited to sites of integrin engagement in *Skap2*$^{-/-}$ BMMs (Fig. 7A). To further test the relationship between Sirpα and Skap2, we determined whether the constitutively active D129K/R140M variant of Skap2 could bypass the requirement for Sirpα to rescue the phenotype rendered by Sirpα deficiency. Unlike Skap2-deficient or Skap2-replete BMMs, *Sirpα*$^{\Delta/\Delta}$ BMMs expressing D129K/R140M Skap2 could not mount a hyperactive cytoskeletal response to integrin stimulation (Fig. 7B). Together, these data demonstrate that Sirpα is required to recruit the Skap2/Adap complex to sites of integrin engagement and, in turn, that recruited Skap2/Adap directs both Sirpα ITIM phosphorylation and downstream actin polymerization.

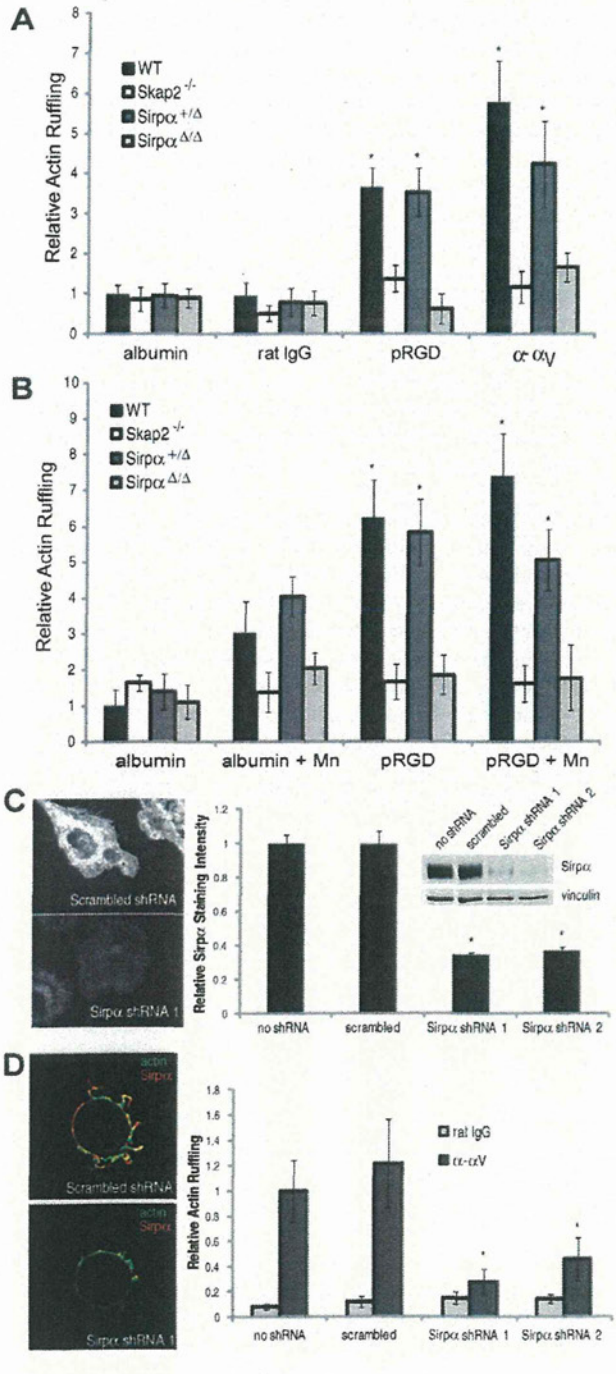

Discussion

This study uncovers a previously unrecognized signaling mechanism required for integrin-mediated signal transduction leading to cytoskeletal reorganization (Fig. 8). Specifically, we show that Skap2 and Sirpα, the latter previously regarded mainly as an inhibitory receptor, are both required for driving integrin-induced cytoskeletal reorganization in macrophages. Our results further indicate that these proteins act in concert – and in proximity to integrins – to transmit signals necessary for the early steps of a novel pathway required for cell migration. Notably, this pathway utilizes a distinct mechanism from IgG- and complement-mediated phagocytosis, which are not affected by the absence of Skap2 and are hyperactive in the absence of Sirpα (Okazawa et al., 2005; Togni et al., 2005). Whereas SFK activation is defective in plated *Skap2*$^{-/-}$ cells, forcing integrins into an active conformation (with Mn^{2+}) stimulates both Syk and SFK activation. However, Mn^{2+} treatment does not restore Adap or Sirpα phosphorylation or integrin-stimulated actin ruffling. Therefore, Syk and SFKs are necessary (Vines et al., 2001), but not sufficient, for integrin-stimulated cytoskeletal rearrangement; their activation via integrin engagement does not obviate the need for Skap2 as a major early mediator downstream of PI3K but upstream of Adap and Sirpα phosphorylation. Skap2 signaling may also be involved in feedback regulation triggered by downstream events including branched actin formation (Coppolino et al., 2001); such a mechanism could be responsible for the Skap2-dependent, plating-induced SFK activation we observed.

Interestingly, Adap is regarded as a driver of inside-out signaling, such as that stimulated by antigen receptor engagement (Wang et al., 2009). However, in our experiments, β1 integrin activation is not dependent on Skap2, the major Adap binding protein. We also find that Mn^{2+}, which promotes the

Fig. 6. Integrin-induced cytoskeletal reorganization is also Sirpα-dependent. (**A**) Actin ruffling induced by beads coated with albumin, rat polyclonal IgG, pRGD, or anti-α_V bound to WT, *Skap2*$^{-/-}$, *Sirpα*$^{+/\Delta}$, and *Sirpα*$^{\Delta/\Delta}$ BMMs. (**B**) Actin ruffling induced by beads coated with albumin or pRGD with or without 1 mM Mn^{2+}. For A and B, data are presented as mean ± S.E.M., n=10 per condition, *P<0.01 compared to either homozygous mutant cell under same conditions. (**C**) Immunofluorescence staining for Sirpα in representative WT BMMs treated with scrambled versus Sirpα shRNA, along with quantified relative staining intensity in untreated cells and cells treated with scrambled shRNA versus the two different Sirpα shRNA. Inset shows western analysis of cell lysates of the same cell populations, blotted for Sirpα. (**D**) Immunofluorescence staining for actin and Sirpα in response to α_V-directed beads on WT BMMs treated with indicated shRNA, along with quantified actin ruffling induced by these beads. Data are presented as mean ± S.E.M., n=10 per condition, *P<0.05 compared to scrambled shRNA and untreated conditions.

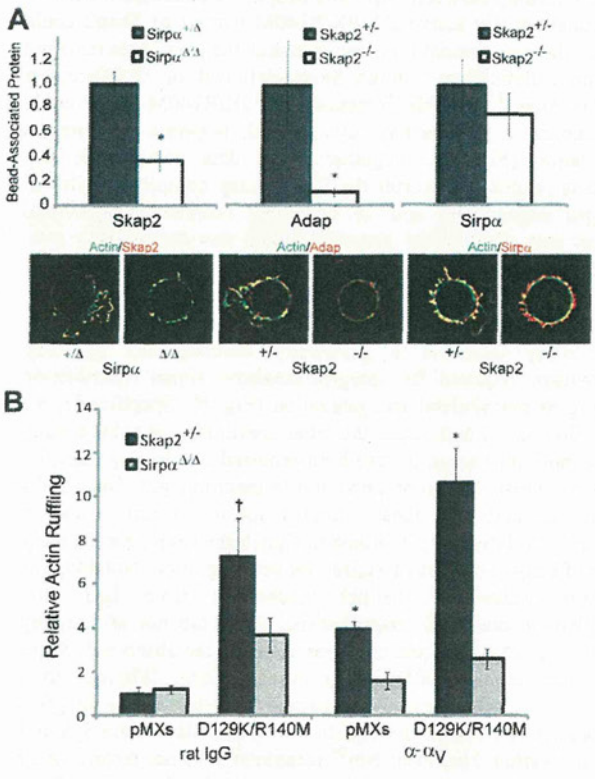

Fig. 7. Sirpα and Skap2 cooperate at sites of integrin engagement to drive cytoskeletal rearrangement. (**A**) Quantified Skap2 recruitment to α–α_V beads bound to *Sirpα*$^{+/\Delta}$ and *Sirpα*$^{\Delta/\Delta}$ BMMs, and Adap and Sirpα recruitment to α–α_V beads bound to *Skap2*$^{+/-}$ and *Skap2*$^{-/-}$ BMMs. Data are normalized to the respective heterozygous condition and presented as mean ± S.E.M., n=10–20 per condition, * P<0.05. Representative beads, co-stained for actin, are shown. (**B**) Actin ruffling induced by beads coated with rat polyclonal IgG or anti-α_V, bound to *Skap2*$^{+/-}$ and *Sirpα*$^{\Delta/\Delta}$ BMMs infected with empty vector (pMXs) or D129K/R140M Skap2. Data are presented as mean ± S.E.M., n=10–15 per condition; † P=0.1 compared to *Sirpα*$^{\Delta/\Delta}$ and P<0.01 compared to pMXs under the same conditions; * P<0.01 compared to *Sirpα*$^{\Delta/\Delta}$ under the same conditions.

general activation of integrins, thus bypassing inside-out pathways, is unable to drive normal actin cytoskeletal responses in *Skap2*$^{-/-}$ BMMs. In these experiments, Mn^{2+} treatment does restore the tyrosyl phosphorylation of selected proteins, consistent with rescue of early integrin functions. Therefore, while we do not exclude the possibility of subtle differences in inside-out signaling in *Skap2*$^{-/-}$ BMMs not detectable by our assays, defects in inside-out integrin signaling pathways are not likely the cause of defective actin ruffling in these cells. Rather, it is clear that additional, Skap2-dependent processes are required to couple early integrin-evoked phosphorylation events to downstream cytoskeletal rearrangements. We propose a model in which a key outside-in integrin-stimulated signal requires the Sirpα/Skap2/Adap complex for actin remodelling in macrophages.

Skap2 is recruited to the plasma membrane by binding Sirpα through a 'back-side' interaction with its C-terminal SH3 domain (Timms et al., 1999). Accordingly, the PH domain is not required to localize Skap2 to the membrane. Instead, interaction between the PH and dimerization domains of Skap2 imposes auto-inhibition that is relieved upon PIP3 binding (Swanson et al., 2008). Consistent with these findings, we report that a Skap2 variant unable to bind PIP3 (R140M) fails to promote integrin-stimulated actin polymerization. Because functional Skap2 homodimerizes, the dominant-negative effect of this variant is likely due to the mutant Skap2 forming hemi-complexes with endogenous Skap2. However, when coupled with a mutation that perturbs the auto-inhibitory binding interface between the PH and dimerization domains, the resulting variant drives hyperactive actin polymerization in response to integrin ligation and in the absence of PIP3 binding. Taken together, these data place Skap2 as an early mediator – just downstream of PI3K but upstream of SFK, Adap and Sirpα – in pathways leading to integrin-driven actin cytoskeletal rearrangement, and also identify the key role of the PH domain in coupling Skap2 activation to phosphoinositide generation.

Prior studies of Skap2, which was discovered as a SFK-associated protein, have provided little mechanistic insight into Skap2 function, aside from its implication in adhesion/migration events (Black et al., 2000; Reinhold et al., 2009; Timms et al., 1999; Togni et al., 2005). The present work provides a mechanistic context in which Skap2 drives integrin-stimulated

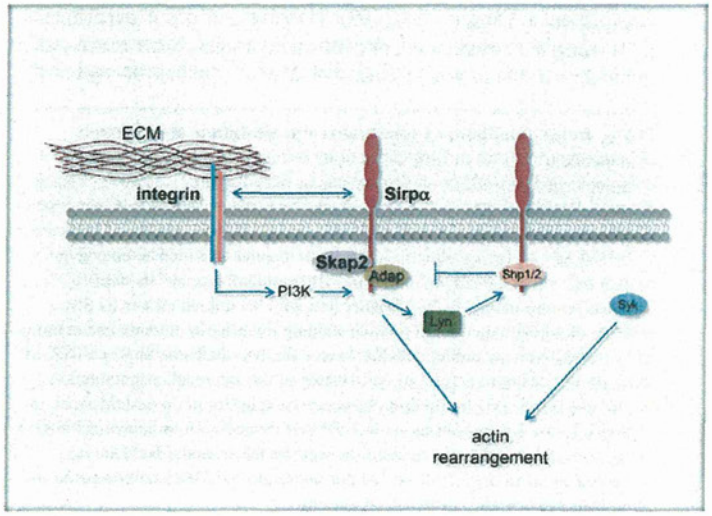

Fig. 8. Skap2 and Sirpα in integrin signaling. A Sirpα/Skap2/Adap signaling module drives actin cytoskeleton reorganization downstream of integrin engagement in macrophages.

cytoskeletal rearrangement. As further support for Skap2's role in normal macrophage biology, it is important to note that the *Yersinia pestis* virulence factor, YopH, targets the Skap2/ADAP complex for dephosphorylation in macrophages as part of its immunosuppressive strategy to interfere with normal adhesion-mediated signaling (Black et al., 2000).

Sirpα is a member of the so-called immune inhibitory receptor family. In addition to binding Skap2, it also binds Shp1/2, and many studies have focused on Shp1/2 interactions with Sirpα's ITIMs to drive negative-regulatory signals (Fujioka et al., 1996). However, we find that both Sirpα and Skap2 are required to transmit signals from ligand-stimulated integrins and to promote local cytoskeletal rearrangement in macrophages. Although there is prior evidence that Sirpα ligation can stimulate nitric oxide pathways (Adams et al., 1998), our finding that Sirpα contributes to integrin outside-in signaling comes as an unexpected and surprising finding, as it demonstrates that Sirpα acts not only as an inhibitory receptor but also as a facilitator of the Skap2-containing pathways downstream of integrin engagement, with significant impact on the cytoskeleton. The findings that Sirpα is recruited to sites of integrin ligation and that a constitutively hyperactive Skap2 mutant cannot salvage actin ruffling in $Sirp\alpha^{\Delta/\Delta}$ BMMs support a mechanism in which Skap2, Adap, and Sirpα cooperate in a single signaling module.

Our results have important implications for understanding the role of Skap2 in inflammatory disorders. For example, Skap2- and Sirpα-deficient mice are resistant to EAE, a mouse model for multiple sclerosis (MS) (Reinhold et al., 2009; Togni et al., 2005; Tomizawa et al., 2007). Both EAE and MS progression depend on antigen-presenting cells such as macrophages, and integrins are an established therapeutic target in MS (Ransohoff, 2007). Additionally, Sirpα-deficient mice are resistant to rheumatoid arthritis, which is partially macrophage-dependent (Okuzawa et al., 2008; Tanaka et al., 2008). We therefore suspect that both Skap2 and Sirpα play important roles in other settings of acute and chronic inflammation, particularly in highly integrin-dependent and macrophage-centric processes such as atherosclerosis and inflammatory bowel disease (Parikh et al., 2012; Rutgeerts et al., 2009; Travis et al., 2007). These roles, along with finer details of downstream signaling promoted by Sirpα and Skap2, are a focus of current and future investigation.

Finally, Sirpα is the receptor for CD47 (Jiang et al., 1999), which constitutes a "don't eat me" signal on both healthy cells and malignant cells evading immune surveillance (Jaiswal et al., 2009; Oldenborg et al., 2001; Takenaka et al., 2007). Although this CD47-driven inhibition has been attributed to the ability of Sirpα to recruit Shp1 to downregulate signals leading to phagocytosis (Oldenborg et al., 2001), our data lead us to speculate that, in addition, CD47 on opposing membranes may interfere with the Sirpα/Skap2 mechanism described here to alter the integrin-mediated cytoskeletal rearrangement necessary for the mechanics of phagocytosis. Therefore, along with the insights the present findings provide on mechanisms of inflammation, our results also could have implications for cancer biology and macrophage-mediated maintenance of homeostasis.

In summary, we have shown that integrin signaling in macrophages involves Sirpα acting via the Skap2/Adap adaptor molecules. Our study significantly changes the current view of integrin outside-in signal transduction in these cells and also provides new insights that could lead to the identification of novel therapeutic targets to regulate both immune surveillance and inflammatory disease.

Materials and Methods

Antibodies and reagents

Anti-pY416 Src, anti-pY118 Paxillin, and anti-pSirpα were obtained from Cell Signaling Technologies. Anti-Pyk2 was purchased from Santa Cruz. Anti-pY352 Syk was purchased from BioSource. 4G10 was a gift from Dr Tom Roberts. Anti-Sirpα and Anti-Adap were purchased from Millipore. Anti-Skap2 was purchased from Proteintech Group. The following integrin antibodies were used in bead assays: RMV7 anti-α_V and 9EG7 anti-β_1 from BD Biosciences, R1-2 anti-α_4, 5H10-27 anti-α_5, M1-70 anti-α_M, M18/2 anti-β_2, and 2C9.G2 anti-β_3 from Biolegend. pRGD and rat polyclonal IgG were purchased from Sigma-Aldrich.

Mice, cell culture, and retroviral gene transduction

Skap2$^{-/-}$ mice (Balb/c) were previously described (Togni et al., 2005), and were maintained under pathogen-free conditions and used at 8–12 weeks. BMMs were differentiated *ex vivo* as described (Tushinski et al., 1982), and analyzed after 7 days in culture. HEK293T/17 cells were maintained in 10% FCS and 10% CO_2 at 37°C. Retroviruses were produced by co-transfecting pEcoPAK (Clonetech) and pMXs-Puro constructs bearing the inserts indicated in the figure legends into HEK293T/17 cells, using polyethylenimine (Polysciences) (Godbey et al., 2000; Swanson et al., 2008). For shRNA knockdown experiments, virus was produced in 296FT cells by co-transfection of the shRNA hairpin in Mission pLKO.1, pCMVD8.9 and p-CMV-VSV-G. shRNA vectors (Sigma-Aldrich) targeted either CTGTCTAACTTCATCCCGAGTT (shRNA 1) or TGGTTCAAAGATGGG-CAAGAA (shRNA 2). Viruses were harvested 36 hours post-infection and used to infect bone marrow cultures, and cells were then differentiated into macrophages in the presence of 2 μM puromycin. All studies were approved by the Institutional Animal Care and Use Committee of Beth Israel Deaconess Medical Center and Harvard Medical School.

Cell migration assays

For modified Boyden-chamber assays, BMMs were suspended in growth media and 5×10^4 cells were placed in transwell chambers (Neuro Probe) with 8-μm pore size and the indicated concentrations of chemokine in the bottom chamber. For chemotaxis to M-CSF, cells were suspended in media containing 10% fetal calf serum. After four hours of incubation, cells were fixed in ethanol, the cells on the upper surface were removed, and the remaining cells on the underside of the membrane were stained with crystal violet and counted subsequent to photomicroscopy at 200×. For wound healing assays, BMMs were plated onto Petri dishes at confluence in growth media and then scratch wounds were introduced into the cultures. The resulting wounds were photographed at 200×, then incubated at 37°C for eight hours and re-photographed.

Bead preparation and binding

10-μm diameter carboxylated polystyrene beads (Polysciences) were washed twice in PBS and mixed with 2 μg of antibody against the specific integrin, rat polyclonal IgG, human serum albumin, or polyRGD overnight at 4°C. This mixture was then washed twice with PBS and blocked with 1% albumin in PBS for 30 minutes. Non-confluent cells plated on No. 1.5 glass coverslips were placed on ice, and beads were added (~10 beads/cell) and allowed to settle onto the cell surface for 10 minutes before returning to 37°C for 20 minutes. For PI3K inhibition, 5 μg/ml GSK2126458 was incubated with cells for 30 minutes prior to bead binding. Cells were washed three times with PBS and then fixed and stained as described below.

Biochemical and FACS analysis

Cells were detached from polystyrene plates by incubation for 30 minutes in Versene (1.5 mM KH_2PO_4, 8 mM Na_2HPO_4, 2.7 mM KCl, 120 mM NaCl, 1 mM glucose, 0.8 mM EDTA) at 4°C. Cells were harvested into DMEM (GibcoBRL), split into equivalent pools and kept in suspension for 2 hours with gentle agitation at room temperature. Equivalent numbers of cells were plated onto polystyrene plates coated with 10 μg/ml bovine fibrinogen for the indicated times and then lysed in Nonidet P-40 (NP-40) lysis buffer (2% NP-40, 100 mM Tris-HCl [pH 7.4], 300 mM NaCl, 200 μM pervanadate, protease inhibitor cocktail [final concentrations, 10 μg/ml leupeptin, 1 μg/ml aprotinin, 1 μg/ml pepstatin, 1 μg/ml antipain]). A sample was also kept in suspension and collected by centrifugation and lysed in lysis buffer. Whole cell extracts were prepared by washing cells in phosphate buffered saline (PBS) and lysing them in NP-40 lysis buffer. Lysates were clarified in a microcentrifuge at 4°C for 10 minutes and protein concentrations in the resulting supernatant were determined using a bicinchoninic acid protein assay reagent kit (Pierce) or Bradford reagent (Biorad). Immunoprecipitations were performed by adding the indicated antibodies and protein A-Sepharose beads to lysates and incubating at 4°C for 2 hr. Immune complexes were washed with lysis buffer, resolved by SDS-PAGE, and transferred

onto Immobilon-FL membranes (Millipore). Immunoblots were blocked with 5% BSA or 5% milk in TBS with 0.05% Triton X-100 (TBST) for 1 hr, incubated for 1 hr with primary antibodies in TBST, washed three times for 10 min each in TBST, then incubated for 1 hr with IR 680-labeled anti-mouse IgG (Invitrogen) or IR 800-labeled anti-rabbit IgG (Rockland, Gilbertsville, PA) and detected using the Li-Cor Odyssey fluorescence reader (Lincoln, NB). FACS analysis for basal integrin expression was performed with the indicated antibodies, and at least 5000 cells per condition were analyzed using FACSCalibur (BD Biosciences). Integrin activation was measured by incubating suspended cells with antibody for 15 minutes at 37°C in the presence or absence of 1.5 nM PMA (Lenter et al., 1993), washing three times, labeling with anti-rat secondary antibody, and performing FACS analysis.

Microscopy

Cells were fixed in 4% PFA, 25 mM PIPES pH 6.8, 129 mM KCl, 20% sucrose, 5 mM EDTA, and permeabilized in 0.05% Triton X-100 in PBS, pH 7.4. For immunofluorescence, cells were stained with phalloidin (Invitrogen), conjugated to either Alexa488 or Alexa568, and rabbit anti-Skap2 (Upstate-Millipore) in 1×PBS containing 3% BSA. Bound antibodies were visualized using Alexa568-conjugated anti-rabbit IgG (Invitrogen) and observed under oil immersion using a Zeiss Axiovert 200 M microscope with a 63×Plan-Apochromat objective with a numerical aperture of 1.4. Confocal images were obtained with a Yokogawa spinning disk on a Nikon Ti inverted microscope equipped with a 60×Plan Apo NA 1.4 objective lens. Fluorescence was excited by 488 nm and 568 nm lines from a 100 mW Melles Griot argon krypton laser. Z-stacks of images 0.5 μm apart, centred at the bead equator, were acquired with a Hamamatsu ORCA ER cooled CCD camera controlled with MetaMorph 7 software. Images were analyzed using the iterative deconvolution program in the Axiovision 4.5 and Metamorph software packages. Using the raw deconvolved images, actin ruffles were quantified in an 8 μm annulus around the bead (excluding the bead itself) at the z-level with largest bead diameter (equator). Brightness and contrast were adjusted on displayed images (identically for compared image sets) using MetaMorph 7 and Adobe Photoshop software.

Statistical testing of differences was performed using the 2-tailed Student's *t*-test.

Acknowledgements

We thank Lewis C. Cantley for his generous support of K.D.S. Microscopy was performed at the Nikon Imaging Center at Harvard Medical School. We are grateful to Yongmei Hu, Bin Zheng and Gregory Finn for their technical help. F.J.A. and K.D.S. designed research, performed research, analyzed data, and wrote the paper. N.T.R. performed research and analyzed data. Q.J.B. and L.I.P. performed research, analyzed data, and assisted in writing the paper. C.A.L., D.E.G., and B.G.N. helped design research and assisted in writing the paper. There are no conflicts of interest to report.

Funding

This work was supported by an American Heart Association Postdoctoral Fellowship to F.J.A. and by the National Institutes of Health [grant numbers NIH T32 HL07604-24 to F.J.A., NIH F31 GM78720 to Q.J.B., NIH R01 HL032854 to D.E.G., NIH GM041890 to L.C.C., NIH R37 CA49132 and R01 CA114945 to B.G.N., and R56AI085131 to K.D.S.]. B.G.N. is a Canada Research Chair, Tier 1, and is partially supported by the Ontario Ministry of Health and the Princess Margaret Hospital Foundation. Deposited in PMC for release after 12 months.

Supplementary material available online at
http://jcs.biologists.org/lookup/suppl/doi:10.1242/jcs.111260/-/DC1

References

Adams, S., van der Laan, L. J., Vernon-Wilson, E., Renardel de Lavalette, C., Döpp, E. A., Dijkstra, C. D., Simmons, D. L. and van den Berg, T. K. (1998). Signal-regulatory protein is selectively expressed by myeloid and neuronal cells. *J. Immunol.* **161**, 1853-1859.

Alenghat, F. J., Tytell, J. D., Thodeti, C. K., Derrien, A. and Ingber, D. E. (2009). Mechanical control of cAMP signaling through integrins is mediated by the heterotrimeric Galphas protein. *J. Cell. Biochem.* **106**, 529-538.

Barclay, A. N. (2009). Signal regulatory protein alpha (SIRPalpha)/CD47 interaction and function. *Curr. Opin. Immunol.* **21**, 47-52.

Berton, G. and Lowell, C. A. (1999). Integrin signaling in neutrophils and macrophages. *Cell. Signal.* **11**, 621-635.

Berzat, A. and Hall, A. (2010). Cellular responses to extracellular guidance cues. *EMBO J.* **29**, 2734-2745.

Black, D. S., Marie-Cardine, A., Schraven, B. and Bliska, J. B. (2000). The Yersinia tyrosine phosphatase YopH targets a novel adhesion-regulated signalling complex in macrophages. *Cell. Microbiol.* **2**, 401-414.

Blaukat, A., Ivankovic-Dikic, I., Grönroos, E., Dolfi, F., Tokiwa, G., Vuori, K. and Dikic, I. (1999). Adaptor proteins Grb2 and Crk couple Pyk2 with activation of specific mitogen-activated protein kinase cascades. *J. Biol. Chem.* **274**, 14893-14901.

Bourette, R. P., Thérier, J. and Mouchiroud, G. (2005). Macrophage colony-stimulating factor receptor induces tyrosine phosphorylation of SKAP55R adaptor and its association with actin. *Cell. Signal.* **17**, 941-949.

Brown, E. J. (1991). Complement receptors and phagocytosis. *Curr. Opin. Immunol.* **3**, 76-82.

Chen, C. S., Alonso, J. L., Ostuni, E., Whitesides, G. M. and Ingber, D. E. (2003). Cell shape provides global control of focal adhesion assembly. *Biochem. Biophys. Res. Commun.* **307**, 355-361.

Coppolino, M. G., Krause, M., Hagendorff, P., Monner, D. A., Trimble, W., Grinstein, S., Wehland, J. and Sechi, A. S. (2001). Evidence for a molecular complex consisting of Fyb/SLAP, SLP-76, Nck, VASP and WASP that links the actin cytoskeleton to Fcgamma receptor signalling during phagocytosis. *J. Cell Sci.* **114**, 4307-4318.

Dransfield, I., Cabañas, C., Craig, A. and Hogg, N. (1992). Divalent cation regulation of the function of the leukocyte integrin LFA-1. *J. Cell Biol.* **116**, 219-226.

Fujioka, Y., Matozaki, T., Noguchi, T., Iwamatsu, A., Yamao, T., Takahashi, N., Tsuda, M., Takada, T. and Kasuga, M. (1996). A novel membrane glycoprotein, SHPS-1, that binds the SH2-domain-containing protein tyrosine phosphatase SHP-2 in response to mitogens and cell adhesion. *Mol. Cell. Biol.* **16**, 6887-6899.

Gahmberg, C. G., Valmu, L., Fagerholm, S., Kotovuori, P., Ihanus, E., Tian, L. and Pessa-Morikawa, T. (1998). Leukocyte integrins and inflammation. *Cell. Mol. Life Sci.* **54**, 549-555.

Geissmann, F., Manz, M. G., Jung, S., Sieweke, M. H., Merad, M. and Ley, K. (2010). Development of monocytes, macrophages, and dendritic cells. *Science* **327**, 656-661.

Godbey, W. T., Barry, M. A., Saggau, P., Wu, K. K. and Mikos, A. G. (2000). Poly(ethylenimine)-mediated transfection: a new paradigm for gene delivery. *J. Biomed. Mater. Res.* **51**, 321-328.

Griffiths, E. K., Krawczyk, C., Kong, Y. Y., Raab, M., Hyduk, S. J., Bouchard, D., Chan, V. S., Kozieradzki, I., Oliveira-Dos-Santos, A. J., Wakeham, A. et al. (2001). Positive regulation of T cell activation and integrin adhesion by the adapter Fyb/Slap. *Science* **293**, 2260-2263.

Hibbs, M. L., Harder, K. W., Armes, J., Kountouri, N., Quilici, C., Casagranda, F., Dunn, A. R. and Tarlinton, D. M. (2002). Sustained activation of Lyn tyrosine kinase *in vivo* leads to autoimmunity. *J. Exp. Med.* **196**, 1593-1604.

Huang, Y., Norton, D. D., Precht, P., Martindale, J. L., Burkhardt, J. K. and Wange, R. L. (2005). Deficiency of ADAP/Fyb/SLAP-130 destabilizes SKAP55 in Jurkat T cells. *J. Biol. Chem.* **280**, 23576-23583.

Hume, D. A. (2006). The mononuclear phagocyte system. *Curr. Opin. Immunol.* **18**, 49-53.

Hynes, R. O. (2002). Integrins: bidirectional, allosteric signaling machines. *Cell* **110**, 673-687.

Inagaki, K., Yamao, T., Noguchi, T., Matozaki, T., Fukunaga, K., Takada, T., Hosooka, T., Akira, S. and Kasuga, M. (2000). SHPS-1 regulates integrin-mediated cytoskeletal reorganization and cell motility. *EMBO J.* **19**, 6721-6731.

Jaiswal, S., Jamieson, C. H., Pang, W. W., Park, C. Y., Chao, M. P., Majeti, R., Traver, D., van Rooijen, N. and Weissman, I. L. (2009). CD47 is upregulated on circulating hematopoietic stem cells and leukemia cells to avoid phagocytosis. *Cell* **138**, 271-285.

Jiang, P., Lagenaur, C. F. and Narayanan, V. (1999). Integrin-associated protein is a ligand for the P84 neural adhesion molecule. *J. Biol. Chem.* **274**, 559-562.

Jo, E. K., Wang, H. and Rudd, C. E. (2005). An essential role for SKAP-55 in LFA-1 clustering on T cells that cannot be substituted by SKAP-55R. *J. Exp. Med.* **201**, 1733-1739.

Johansen, M. L. and Brown, E. J. (2007). Dual regulation of SIRPalpha phosphorylation by integrins and CD47. *J. Biol. Chem.* **282**, 24219-24230.

Jones, G. E. (2000). Cellular signaling in macrophage migration and chemotaxis. *J. Leukoc. Biol.* **68**, 593-602.

Kasirer-Friede, A., Moran, B., Nagrampa-Orje, J., Swanson, K., Ruggeri, Z. M., Schraven, B., Neel, B. G., Koretzky, G. and Shattil, S. J. (2007). ADAP is required for normal alphaIIbbeta3 activation by VWF/GP Ib-IX-V and other agonists. *Blood* **109**, 1018-1025.

Kharitonenkov, A., Chen, Z., Sures, I., Wang, H., Schilling, J. and Ullrich, A. (1997). A family of proteins that inhibit signalling through tyrosine kinase receptors. *Nature* **386**, 181-186.

Kouroku, Y., Soyama, A., Fujita, E., Urase, K., Tsukahara, T. and Momoi, T. (1998). RA70 is a src kinase-associated protein expressed ubiquitously. *Biochem. Biophys. Res. Commun.* **252**, 738-742.

Lenter, M., Uhlig, H., Hamann, A., Jenö, P., Imhof, B. and Vestweber, D. (1993). A monoclonal antibody against an activation epitope on mouse integrin chain beta 1 blocks adhesion of lymphocytes to the endothelial integrin alpha 6 beta 1. *Proc. Natl. Acad. Sci. USA* **90**, 9051-9055.

Leung, E., Kim, J. E., Rewcastle, G. W., Finlay, G. J. and Baguley, B. C. (2011). Comparison of the effects of the PI3K/mTOR inhibitors NVP-BEZ235 and GSK2126458 on tamoxifen-resistant breast cancer cells. *Cancer Biol. Ther.* **11**, 938-946.

Liu, J., Kang, H., Raab, M., da Silva, A. J., Kraeft, S. K. and Rudd, C. E. (1998). FYB (FYN binding protein) serves as a binding partner for lymphoid protein and FYN kinase substrate SKAP55 and a SKAP55-related protein in T cells. *Proc. Natl. Acad. Sci. USA* **95**, 8779-8784.

Marie-Cardine, A., Hendricks-Taylor, L. R., Boerth, N. J., Zhao, H., Schraven, B. and Koretzky, G. A. (1998). Molecular interaction between the Fyn-associated protein SKAP55 and the SLP-76-associated phosphoprotein SLAP-130. *J. Biol. Chem.* **273**, 25789-25795.

Miyamoto, S., Akiyama, S. K. and Yamada, K. M. (1995). Synergistic roles for receptor occupancy and aggregation in integrin transmembrane function. *Science* **267**, 883-885.

Moog-Lutz, C., Peterson, E. J., Lutz, P. G., Eliason, S., Cavé-Riant, F., Singer, A., Di Gioia, Y., Dmowski, S., Kamens, J., Cayre, Y. E. et al. (2001). PRAM-1 is a novel adaptor protein regulated by retinoic acid (RA) and promyelocytic leukemia (PML)-RA receptor alpha in acute promyelocytic leukemia cells. *J. Biol. Chem.* **276**, 22375-22381.

Motegi, S., Okazawa, H., Ohnishi, H., Sato, R., Kaneko, Y., Kobayashi, H., Tomizawa, K., Ito, T., Honma, N., Bühring, H. J. et al. (2003). Role of the CD47-SHPS-1 system in regulation of cell migration. *EMBO J.* **22**, 2634-2644.

Okazawa, H., Motegi, S., Ohyama, N., Ohnishi, H., Tomizawa, T., Kaneko, Y., Oldenborg, P. A., Ishikawa, O. and Matozaki, T. (2005). Negative regulation of phagocytosis in macrophages by the CD47-SHPS-1 system. *J. Immunol.* **174**, 2004-2011.

Okuzawa, C., Kaneko, Y., Murata, Y., Miyake, A., Saito, Y., Okajo, J., Tomizawa, T., Kaneko, Y., Okazawa, H., Ohnishi, H. et al. (2008). Resistance to collagen-induced arthritis in SHPS-1 mutant mice. *Biochem. Biophys. Res. Commun.* **371**, 561-566.

Oldenborg, P. A., Gresham, H. D. and Lindberg, F. P. (2001). CD47-signal regulatory protein alpha (SIRPalpha) regulates Fcgamma and complement receptor-mediated phagocytosis. *J. Exp. Med.* **193**, 855-862.

Parikh, A., Leach, T., Wyant, T., Scholz, C., Sankoh, S., Mould, D. R., Ponich, T., Fox, I. and Feagan, B. G. (2012). Vedolizumab for the treatment of active ulcerative colitis: a randomized controlled phase 2 dose-ranging study. *Inflamm. Bowel Dis.* **18**, 1470-1479.

Peters, M. A., Wendholt, D., Strietholt, S., Frank, S., Pundt, N., Korb-Pap, A., Joosten, L. A., van den Berg, W. B., Kollias, G., Eckes, B. et al. (2012). The loss of α2β1 integrin suppresses joint inflammation and cartilage destruction in mouse models of rheumatoid arthritis. *Arthritis Rheum.* **64**, 1359-1368.

Plow, E. F., Haas, T. A., Zhang, L., Loftus, J. and Smith, J. W. (2000). Ligand binding to integrins. *J. Biol. Chem.* **275**, 21785-21788.

Ransohoff, R. M. (2007). Natalizumab for multiple sclerosis. *N. Engl. J. Med.* **356**, 2622-2629.

Reinhold, A., Reimann, S., Reinhold, D., Schraven, B. and Togni, M. (2009). Expression of SKAP-HOM in DCs is required for an optimal immune response *in vivo*. *J. Leukoc. Biol.* **86**, 61-71.

Rutgeerts, P., Vermeire, S. and Van Assche, G. (2009). Biological therapies for inflammatory bowel diseases. *Gastroenterology* **136**, 1182-1197.

Swanson, K. D., Tang, Y., Ceccarelli, D. F., Poy, F., Sliwa, J. P., Neel, B. G. and Eck, M. J. (2008). The Skap-hom dimerization and PH domains comprise a 3′-phosphoinositide-gated molecular switch. *Mol. Cell* **32**, 564-575.

Takenaka, K., Prasolava, T. K., Wang, J. C., Mortin-Toth, S. M., Khalouei, S., Gan, O. I., Dick, J. E. and Danska, J. S. (2007). Polymorphism in Sirpa modulates engraftment of human hematopoietic stem cells. *Nat. Immunol.* **8**, 1313-1323.

Tanaka, K., Horikawa, T., Suzuki, S., Kitaura, K., Watanabe, J., Gotoh, A., Shiobara, N., Itoh, T., Yamane, S., Suzuki, R. et al. (2008). Inhibition of Src homology 2 domain-containing protein tyrosine phosphatase substrate-1 reduces the severity of collagen-induced arthritis. *J. Rheumatol.* **35**, 2316-2324.

Timms, J. F., Swanson, K. D., Marie-Cardine, A., Raab, M., Rudd, C. E., Schraven, B. and Neel, B. G. (1999). SHPS-1 is a scaffold for assembling distinct adhesion-regulated multi-protein complexes in macrophages. *Curr. Biol.* **9**, 927-930.

Togni, M., Swanson, K. D., Reimann, S., Kliche, S., Pearce, A. C., Simeoni, L., Reinhold, D., Wienands, J., Neel, B. G., Schraven, B. et al. (2005). Regulation of *in vitro* and *in vivo* immune functions by the cytosolic adaptor protein SKAP-HOM. *Mol. Cell. Biol.* **25**, 8052-8063.

Tomizawa, T., Kaneko, Y., Kaneko, Y., Saito, Y., Ohnishi, H., Okajo, J., Okuzawa, C., Ishikawa-Sekigami, T., Murata, Y., Okazawa, H. et al. (2007). Resistance to experimental autoimmune encephalomyelitis and impaired T cell priming by dendritic cells in Src homology 2 domain-containing protein tyrosine phosphatase substrate-1 mutant mice. *J. Immunol.* **179**, 869-877.

Travis, M. A., Reizis, B., Melton, A. C., Masteller, E., Tang, Q., Proctor, J. M., Wang, Y., Bernstein, X., Huang, X., Reichardt, L. F. et al. (2007). Loss of integrin alpha(v)beta8 on dendritic cells causes autoimmunity and colitis in mice. *Nature* **449**, 361-365.

Tushinski, R. J., Oliver, I. T., Guilbert, L. J., Tynan, P. W., Warner, J. R. and Stanley, E. R. (1982). Survival of mononuclear phagocytes depends on a lineage-specific growth factor that the differentiated cells selectively destroy. *Cell* **28**, 71-81.

Veillette, A., Thibaudeau, E. and Latour, S. (1998). High expression of inhibitory receptor SHPS-1 and its association with protein-tyrosine phosphatase SHP-1 in macrophages. *J. Biol. Chem.* **273**, 22719-22728.

Vicente-Manzanares, M. and Sánchez-Madrid, F. (2004). Role of the cytoskeleton during leukocyte responses. *Nat. Rev. Immunol.* **4**, 110-122.

Vines, C. M., Potter, J. W., Xu, Y., Geahlen, R. L., Costello, P. S., Tybulewicz, V. L., Lowell, C. A., Chang, P. W., Gresham, H. D. and Willman, C. L. (2001). Inhibition of beta 2 integrin receptor and Syk kinase signaling in monocytes by the Src family kinase Fgr. *Immunity* **15**, 507-519.

Wang, H., Wei, B., Bismuth, G. and Rudd, C. E. (2009). SLP-76-ADAP adaptor module regulates LFA-1 mediated costimulation and T cell motility. *Proc. Natl. Acad. Sci. USA* **106**, 12436-12441.

Williams, L. M. and Ridley, A. J. (2000). Lipopolysaccharide induces actin reorganization and tyrosine phosphorylation of Pyk2 and paxillin in monocytes and macrophages. *J. Immunol.* **164**, 2028-2036.

Worthylake, R. A. and Burridge, K. (2001). Leukocyte transendothelial migration: orchestrating the underlying molecular machinery. *Curr. Opin. Cell Biol.* **13**, 569-577.

Yakubenko, V. P., Lishko, V. K., Lam, S. C. and Ugarova, T. P. (2002). A molecular basis for integrin alphaMbeta 2 ligand binding promiscuity. *J. Biol. Chem.* **277**, 48635-48642.

Journal of Cell Science

Cell PRESS
Open ACCESS

Cell Reports
Report

SIRPα Controls the Activity of the Phagocyte NADPH Oxidase by Restricting the Expression of gp91^{phox}

Ellen M. van Beek,[1,4] Julian Alvarez Zarate,[1,4] Robin van Bruggen,[1] Karin Schornagel,[1] Anton T.J. Tool,[1] Takashi Matozaki,[2] Georg Kraal,[3] Dirk Roos,[1] and Timo K. van den Berg[1,*]

[1]Sanquin Research and Landsteiner Laboratory, Academic Medical Center, University of Amsterdam, 1066 CX, Amsterdam, The Netherlands
[2]Division of Molecular and Cellular Signaling, Department of Biochemistry and Molecular Biology, Kobe University Graduate School of Medicine, Kobe 650-0017, Japan
[3]Department of Molecular Cell Biology and Immunology, VU Medical Center, 1081 BT, Amsterdam, The Netherlands
[4]These authors contributed equally to this work
*Correspondence: t.k.vandenberg@sanquin.nl
http://dx.doi.org/10.1016/j.celrep.2012.08.027

SUMMARY

The phagocyte NADPH oxidase mediates oxidative microbial killing in granulocytes and macrophages. However, because the reactive oxygen species produced by the NADPH oxidase can also be toxic to the host, it is essential to control its activity. Little is known about the endogenous mechanism(s) that limits NADPH oxidase activity. Here, we demonstrate that the myeloid-inhibitory receptor SIRPα acts as a negative regulator of the phagocyte NADPH oxidase. Phagocytes isolated from SIRPα mutant mice were shown to have an enhanced respiratory burst. Furthermore, overexpression of SIRPα in human myeloid cells prevented respiratory burst activation. The inhibitory effect required interactions between SIRPα and its natural ligand, CD47, as well as signaling through the SIRPα cytoplasmic immunoreceptor tyrosine-based inhibitory motifs. Suppression of the respiratory burst by SIRPα was caused by a selective repression of gp91^{phox} expression, the catalytic component of the phagocyte NADPH oxidase complex. Thus, SIRPα can limit gp91^{phox} expression during myeloid development, thereby controlling the magnitude of the respiratory burst in phagocytes.

INTRODUCTION

One of the most important antimicrobial activities of phagocytes is the abrupt formation of reactive oxygen species (ROS), a process known as the respiratory burst. This is mediated by the phagocyte NADPH oxidase complex, and its importance is best illustrated by patients with chronic granulomatous disease (CGD) and dysfunctional NADPH oxidase, and as a result are hypersusceptible to a variety of bacterial and fungal infections (Roos et al., 2003; Bedard and Krause, 2007). The phagocyte NADPH oxidase is a multisubunit enzyme complex composed of (1) the membrane proteins gp91^{phox} (NOX2, the catalytic component of the oxidase) and p22^{phox}; (2) the cytosolic proteins p40^{phox}, p47^{phox}, and p67^{phox}; and (3) the small GTPase Rac. Activation of the oxidase involves translocation of the cytosolic subunits p40^{phox}, p47^{phox}, p67^{phox}, and Rac to the plasma membrane and assembly of the oxidase complex. Once assembled, the NADPH oxidase generates superoxide (O_2^-) formation by transferring electrons from NADPH in the cytosol over the plasma membrane to molecular oxygen. Superoxide produced by the oxidase forms the basic compound from which other ROS, such as hydrogen peroxide (H_2O_2) and hypochlorous acid (HOCl), are formed. High concentrations of ROS are directly toxic to microbes, and may also be indirectly toxic due to the liberation of hydrolytic proteases (Reeves et al., 2002).

The mechanisms of NADPH oxidase activation have been relatively well characterized, but essentially nothing is known about whether and how the magnitude of the respiratory burst is controlled. The latter is important because ROS not only play a critical role in host defense but can also be toxic to the host. The tight control over NADPH oxidase activity is illustrated in part by the observation that there is only very little interindividual variation in the respiratory burst (Zhao et al., personal communication). The magnitude of the respiratory burst is likely to be primarily determined by the protein expression levels of the various NADPH oxidase components, which are expressed in a developmentally regulated fashion in phagocytes. Although the developmental pathways and transcription factors that trigger the expression of the different NADPH oxidase components during myeloid development have been established (Lindsey et al., 2007; Zhu et al., 2008; Kautz et al., 2001), the putative regulatory mechanisms that counterbalance these factors and prevent excessive, potentially harmful expression of the various NADPH oxidase components within phagocytes have remained unknown.

SIRPα is an inhibitory immunoreceptor that is predominantly expressed on myeloid and neuronal cells (Fujioka et al., 1996; Adams et al., 1998). The cytoplasmic region of SIRPα contains four immunoreceptor tyrosine-based inhibitory motifs (ITIMs) that upon ligand binding become phosphorylated and mediate the recruitment and activation of the SH2-domain-containing

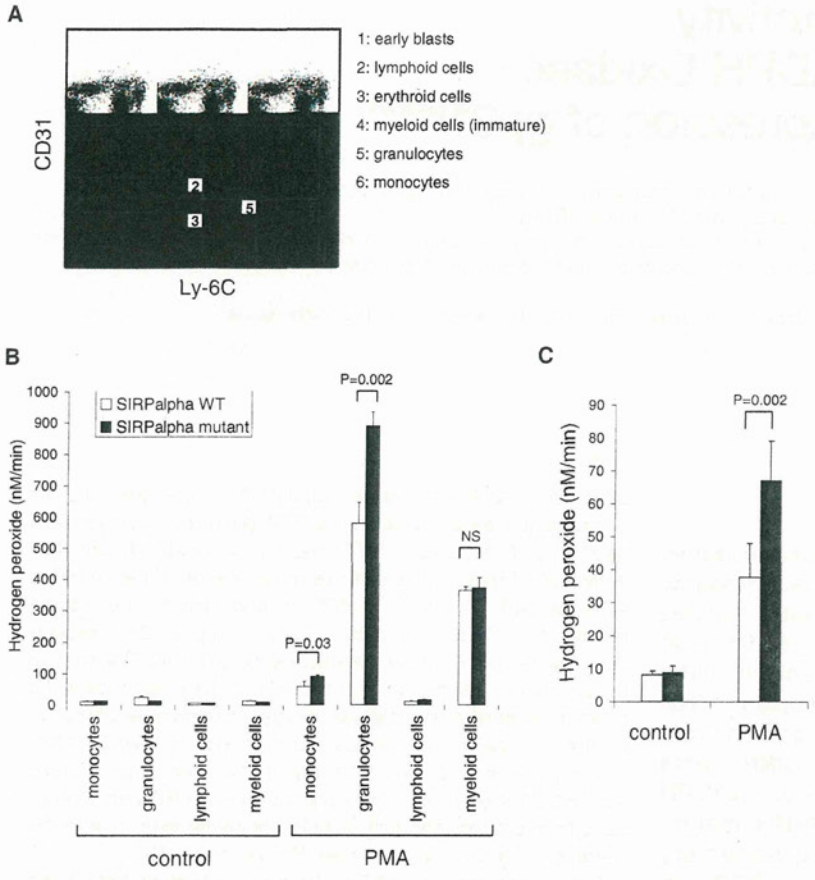

Figure 1. Phagocyte NADPH Oxidase Activity Is Enhanced in Macrophages and Granulocytes from SIRPα Mutant Mice

(A) Flow-cytometric double labeling of bone-marrow cells for CD31 and Ly-6C, identifying the major subpopulations of hematopoietic cells.

(B and C) Sorted populations of (B) monocytes, granulocytes, lymphocytes, and immature myeloid cells, or (C) cultured bone-marrow-derived macrophages from WT (white bars) or SIRPα mutant (black bars) C57BL/6 mice were evaluated for PMA-induced NADPH oxidase activity.

Data are the means ± SD of five animals, with each measurement performed in triplicate. Significance was determined by Student's t test. See also Figure S1.

tyrosine phosphatases (PTPase) SHP-1 and SHP-2. SHP-1 and SHP-2 can in turn dephosphorylate specific protein substrates and thereby mediate various biological functions, generally in a negative fashion. The N-terminal V-like Ig domain mediates recognition of the broadly expressed transmembrane glycoprotein CD47 (Jiang et al., 1999; Seiffert et al., 1999; Vernon-Wilson et al., 2000; Liu et al., 2007; Lee et al., 2007; Hatherley et al., 2008). SIRPα has been implicated in the regulation of a number of functions in myeloid cells (van Beek et al., 2005; Barclay and Brown, 2006). One of the best-documented functions of SIRPα is its inhibitory role in the phagocytosis of host cells by macrophages. In particular, the ligation of SIRPα on macrophages by the "don't eat me" signal CD47 expressed on host cells, such as erythrocytes and platelets, generates an inhibitory signal that negatively regulates phagocytosis (Oldenborg et al., 2000; Yamao et al., 2002). This suggests that CD47 acts as a molecular signature of self that limits immune-mediated damage against normal and healthy host cells during infection and inflammation by interacting with the self sensor SIRPα on phagocytes and other myeloid cells. However, until now, a direct involvement of CD47-SIRPα interactions in the regulation of inflammatory mediators and antimicrobial functions has not been reported.

Here we demonstrate that SIRPα acts as a critical negative regulator of the respiratory burst. Inhibition of the phagocyte NADPH oxidase by SIRPα involves interactions between SIRPα and the self molecule CD47, as well as signaling through the SIRPα ITIMs, which result in a selective suppression of gp91^{phox} expression. This mechanism may help prevent collateral oxidative damage to the host during infection and other inflammatory conditions.

RESULTS AND DISCUSSION

Enhanced NADPH Oxidase Activity in SIRPα Mutant Phagocytes

To investigate whether SIRPα signaling regulates the phagocyte NADPH oxidase, we performed studies with cells from SIRPα mutant mice. These mice express a SIRPα molecule lacking the cytoplasmic tail and signaling capacity (Yamao et al., 2002). We sorted distinct bone-marrow cell populations of SIRPα mutant and control mice, including granulocytes, monocytes, immature myeloid cells, and lymphoid cells, by fluorescence-activated cell sorting (FACS) using CD31 and Ly-6C as markers (Figure 1A) as described previously (Nikolic et al., 2003), and analyzed their phorbol myristate acetate (PMA)-induced respiratory burst. As reported previously (van Beek et al., 2009), there were no detectable differences in bone-marrow composition between the mutant and control mice, essentially excluding a prominent nonredundant role of SIRPα signaling in myeloid differentiation. We observed a significantly (50%–75%) enhanced respiratory burst activity in granulocytes and monocytes from SIRPα mutant mice in comparison with cells from wild-type (WT) mice (Figure 1B). A similar difference was seen in bone-marrow-derived macrophages (Figure 1C). The respiratory burst in immature myeloid cells (Figure 1B) appeared unaffected. A comparison of WT and SIRPα mutant mice showed that the production of other inflammatory mediators, including nitric oxide (NO), tumor necrosis factor α (TNFα), interleukin 1β (IL1β), IL6, and IL10, by bone-marrow-derived macrophages in response to lipopolysaccharide (LPS) was not significantly affected (Figure S1). Collectively,

these data indicate a selective inhibitory role for SIRPα signaling in the regulation of the respiratory burst.

The lack of difference between WT and SIRPα mutant phagocytes appears to be in contrast to previous reports (Kong et al., 2007; Dong et al., 2008), in which knockdown of SIRPα in macrophages was shown to enhance cytokine production in response to TLR ligands. A possible explanation for this apparent discrepancy is that inhibition of cytokine production can only be caused by a complete absence of SIRPα, and not by selective deletion of its cytoplasmic tail. A more trivial explanation could relate to differences in the method used for interference. We used macrophages from gene-targeted knockout mice, whereas the other studies used small hairpin RNA (shRNA)- and small interfering RNA (siRNA)-mediated knockdown, which may have triggered macrophage danger pathways that contributed to the response (Stacey et al., 2000). Our current findings essentially exclude a regulatory role for SIRPα signaling in TLR-induced cytokine production, and support the idea that SIRPα signaling regulates selected inflammatory mediators, such as ROS.

SIRPα Overexpression Inhibits the NADPH Oxidase in Human Phagocytic Cells

To investigate the mechanism by which SIRPα regulates the phagocyte respiratory burst, we tested the effect of overexpression of SIRPα in human myeloid PLB-985 cells. PLB-985 cells are suitable for studying NADPH oxidase activity (Zhen et al., 1993), and were found to express relatively low levels of endogenous SIRPα as shown by western blotting (Figure S2A) and flow cytometry (Figure S4A). A chimeric rat-human SIRPα protein was expressed in PLB-985 cells because it allows for selective monitoring and manipulation by the agonistic monoclonal antibody (mAb) ED9 specifically directed against the rat SIRPα extracellular domain (Adams et al., 1998; Alblas et al., 2005). PLB-985 cells, or mutants with a targeted mutation of the gp91^{phox} gene (PLB-985 X-CGD; Zhen et al., 1993), were retrovirally transduced with full-length chimeric rat-human SIRPα protein (SIRPα-WT) or a SIRPα deletion mutant (SIRPα-Δ87) that is unable to signal because it lacks the cytoplasmic tail. A flow-cytometric analysis showed that the levels of SIRPα expression were comparable for the different cell lines generated (Figure 2A) and similar to those generally seen in rat myeloid cell lines or primary rat myeloid cells, such as macrophages or granulocytes (Adams et al., 1998; not shown). Western blotting with an antibody against the cytoplasmic tail of SIRPα identified both endogenous and chimeric SIRPα proteins, and confirmed that SIRPα-Δ87 cells express a truncated SIRPα (Figure S2A).

We studied the respiratory burst in the different PLB-985 cells after in vitro granulocytic or monocytic differentiation using dimethylformamide (DMF) or vitamin D3 (VitD3), respectively. PMA-induced NADPH oxidase activity was normal in control cells but was abolished in cells expressing WT SIRPα (Figures 2B and 2C). This effect occurred after either granulocytic or monocytic differentiation. Clearly, the inhibitory effect was not observed in the SIRPα-Δ87 mutant, suggesting that SIRPα signaling was required. In fact, the SIRPα-Δ87 cells generated a considerably higher response than the empty vector cells, suggesting that the mutant SIRPα protein acted as a dominant-negative protein by competing with, e.g., endogenous SIRPα for CD47 binding (see below). Of importance, all responses were entirely attributable to the gp91^{phox} (NOX2)-containing phagocyte NADPH oxidase, because they were completely absent in the PLB-985 X-CGD cells, which have a targeted mutation of the gp91^{phox}-encoding *CYBB* gene. Among several other tested stimuli of NADPH oxidase activation (i.e., serum-treated zymosan [STZ], formyl-methionyl-leucyl-phenylalanine [fMLP], and human IgG complexes), only STZ generated a measurable response in the PLB-985 cells, and again this was completely abrogated by SIRPα-WT expression (Figure S2B). This is consistent with a generalized effect of SIRPα on the NADPH oxidase.

SIRPα Selectively Represses gp91^{phox} Expression during Myeloid Differentiation

Activation of the multisubunit NADPH oxidase complex requires assembly of its individual components, which are expressed during myeloid differentiation (Roos et al., 2003). To establish the basis for SIRPα-dependent regulation of the respiratory burst, we investigated the expression levels of the different components of the NADPH oxidase complex upon myeloid differentiation. Expression of the membrane component gp91^{phox}, which forms the enzymatic core of the phagocyte NADPH oxidase, was evaluated in undifferentiated or granulocytic or monocytic differentiated PLB-985 cells by western blotting. The differentiation-induced rise in gp91^{phox} expression was completely absent in cells that express the full-length SIRPα protein (SIRPα-WT; Figure 2D). The same was observed when surface levels of gp91^{phox} were analyzed by flow cytometry with 7D5 mAb (Figure S3A). Also, the enhanced respiratory burst activity in cells that express the truncated receptor (SIRPα-Δ87) was associated with a higher gp91^{phox} expression. Of importance, the levels of two other NADPH oxidase components, p67^{phox} and p47^{phox}, remained unaffected by overexpression of full-length or truncated SIRPα (Figure 2D), suggesting that SIRPα was selectively regulating gp91^{phox} expression. However, the similar levels of upregulation of p47 and p67 observed in the empty vector, SIRPα-WT, and SIRPα-Δ87 cells also indicated that differentiation was unaffected by the introduction of SIRPα-WT or SIRPα-Δ87, suggesting that SIRPα was not regulating differentiation in general. Furthermore, SIRPα did not affect the upregulation of other myeloid differentiation markers, such as CD11b and CD14, during granulocytic or monocytic differentiation (not shown). The upregulation of endogenous SIRPα on PLB-985 cells coincided with that of gp91^{phox} at days 1–3 of neutrophilic differentiation (Figure S3B).

To demonstrate that gp91^{phox} was indeed the only relevant factor downregulated by SIRPα, gp91^{phox} was reconstituted by retroviral expression into SIRPα-WT cells (Figure 2E), and this resulted in a full restoration of the respiratory burst (Figure 2F). A similar restoration was observed when such reconstitution was performed in PLB-985 X-CGD cells. This shows that SIRPα suppresses phagocyte NADPH oxidase activity by a selective repression of gp91^{phox} protein expression during myeloid differentiation.

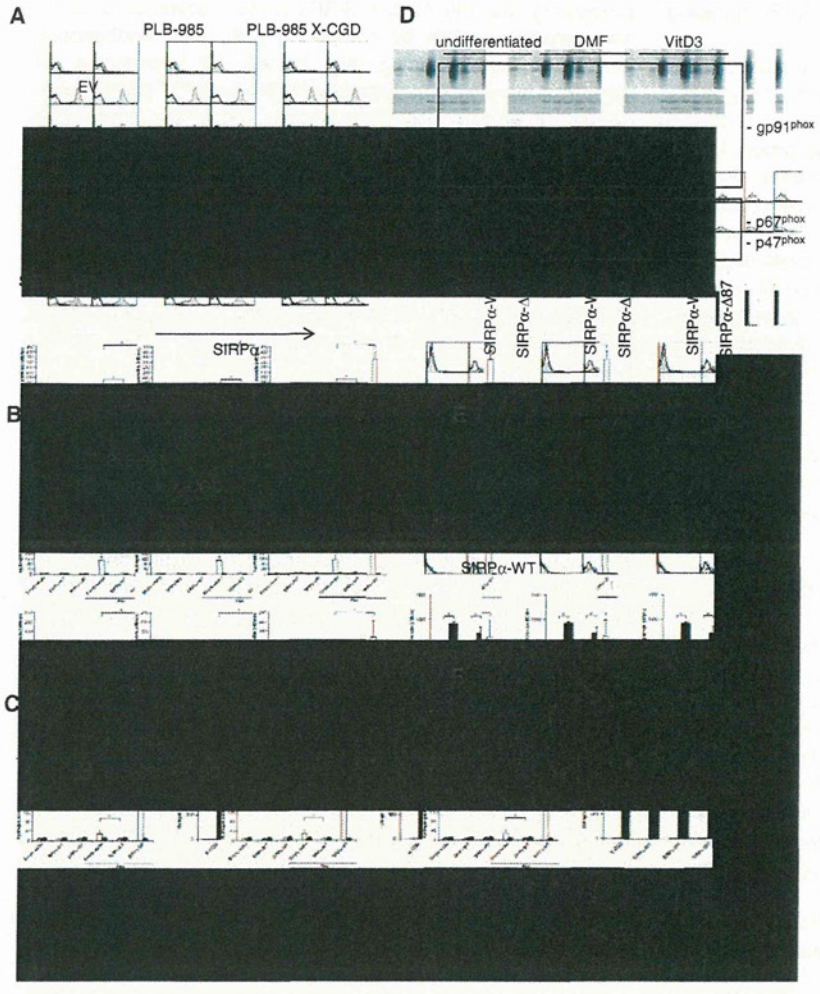

Figure 2. SIRPα Overexpression in PLB-985 Cells Inhibits the Respiratory Burst by Repressing gp91^{phox} Expression

PLB-985 and gp91^{phox} PLB-985 X-CGD cells were stably transduced with empty vector, chimeric rat-human SIRPα (SIRPα-WT), or an N-terminal truncated SIRPα protein lacking 87 amino acids of the cytoplasmic tail of SIRPα (SIRPα-Δ87).

(A) SIRPα surface expression was evaluated by flow cytometry with Alexa 633-conjugated ED9 directed against rat SIRPα antibody (solid histograms). Unstained cells are indicated as control (open histogram).

(B and C) PMA-induced NADPH-oxidase activity in the indicated PLB-985 (white bars) and PLB-985 X-CGD (black bars) cell lines after 5–6 days of either granulocytic (B) or monocytic (C) differentiation induced with DMF or VitD3, respectively. Values shown in (B) and (C) represent means ± SD of 15 measurements from five independent experiments; *p < 0.001, by Student's t test.

(D) Expression levels of gp91^{phox}, p67^{phox}, and p47^{phox} determined by western blotting in undifferentiated PLB-985 cells or those differentiated with DMF or vitamin D3 into granulocytic or monocytic cells, respectively. Note the lack of gp91^{phox}, but not p67^{phox} or p47^{phox}, in SIRPα-WT cells.

(E) Restoration of gp91^{phox} expression after reconstitution of gp91^{phox} in SIRPα-WT and X-CGD empty vector cells by retroviral transduction. The expression of gp91^{phox} before (left panel) and after (right panel) retroviral transduction was evaluated by flow cytometry after incubation with mAb 7D5 and goat-anti-mouse-IgG1 Alexa 633 antibody (solid histogram) or stained with isotype-matched antibody (open histogram).

(F) PMA-induced NADPH-oxidase activity in granulocytic SIRPα-WT and X-CGD empty vector cells (white bars) in which gp91^{phox} was reconstituted (black bars).

Data are presented as the mean ± SD of three independent experiments each performed in triplicate; *p < 0.001, by Student's t test. See also Figures S2 and S3.

Inhibition of the NADPH Oxidase Involves Signaling via the SIRPα Cytoplasmic ITIMs

The experiments described above suggested that direct signaling through the cytoplasmic tail is involved in the regulation of the NADPH oxidase and gp91^{phox} protein expression. The SIRPα cytoplasmic tail harbors ITIMs responsible for the recruitment of the cytosolic tyrosine phosphatases SHP-1 and SHP-2 (Fujioka et al., 1996). Studies with dominant-negative SHP-1 in myeloid cells (Dong et al., 1999) and with phagocytes from *motheaten* SHP-1-deficient mice (Kruger et al., 2000) demonstrated that at least SHP-1 acts as a negative regulator of the respiratory burst in myeloid cells. To investigate whether SHP-1 and/or SHP-2 recruitment by SIRPα plays a critical role in suppressing the respiratory burst by SIRPα, we mutated each of the four tyrosines from the SIRPα ITIMs, or combinations thereof, into phenylalanines and expressed the resultant proteins in PLB-985 cells. To evaluate the binding of SHP-1 and SHP-2 to the SIRPα mutants, we performed immunoprecipitation experiments. An analysis of the precipitates by western blotting demonstrated constitutive binding of SHP-1 and SHP-2 to SIRPα, and this was eliminated or at least strongly reduced by mutation of the ITIM tyrosines (Figure 3A). The same was observed in the reverse experiment, i.e., SHP-1 or SHP-2 immunoprecipitation followed by western blotting with SIRPα specific antibody (not shown). Mutation of all four ITIM tyrosines (SIRPα-Y1, SIRPα-Y2, SIRPα-Y3, and SIRPα-Y4F) completely restored the respiratory burst (Figure 3B) and gp91^{phox} protein expression (Figure 3C) to levels seen with the SIRPα-Δ87 cytoplasmic deletion mutant, suggesting that the ITIMs were responsible for the inhibitory activity. The level of inhibition obtained with the individual mutants correlated very well with their capacity to recruit SHP-1 and SHP-2. For instance, the membrane proximal Y1 appeared to be more important for the negative regulation of the NADPH oxidase than its membrane distal counterpart Y3.

To obtain insight into the level of gp91^{phox} regulation by SIRPα, we analyzed its mRNA levels by quantitative PCR (qPCR) in the various PLB-985 mutants. Similarly to the gp91^{phox} protein

Cell PRESS
Open ACCESS

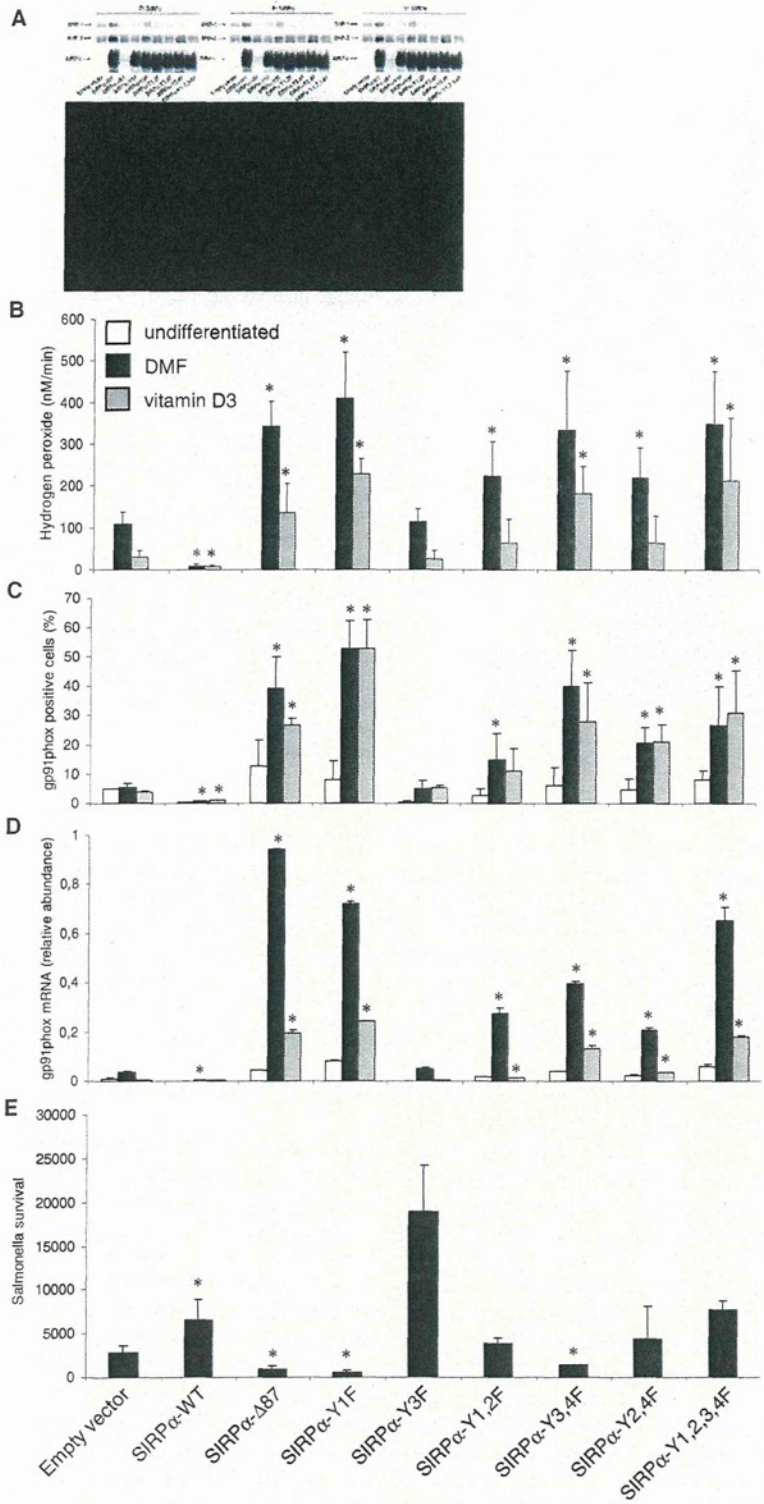

Figure 3. The Cytoplasmic ITIMs of SIRPα Are Required for Inhibition of the NADPH Oxidase

(A) SHP-1 and SHP-2 binding to SIRPα-WT, SIRPα-Δ87, and SIRPα tyrosine mutants was evaluated by immunoprecipitation of SIRPα, with mAb ED9 against rat SIRPα, and western blotting with antibodies against SHP-1, SHP-2, and SIRPα.

(B) PMA-induced NADPH oxidase activity in differentiated granulocytic or monocytic PLB-985. Data are presented as the mean ± SD of three independent experiments, each performed in triplicate.

(C) Expression of surface gp91^{phox} in differentiated granulocytic or monocytic, or undifferentiated PLB-985 cells analyzed by flow cytometry using 7D5 mAb. Data are presented as the mean ± SD of three independent experiments.

(D) mRNA level of gp91^{phox} in granulocytic or monocytic differentiated, or undifferentiated cells detected by RT-qPCR. Data are presented as the mean ± SD of two independent experiments, each performed in duplicate.

(E) Intracellular killing of *Salmonella* bacteria. The different cell lines were allowed to ingest *S. enterica* serovar Typhimurium 14028s, and the numbers of intracellular bacteria were determined 24 h after challenge. The levels of *Salmonella* uptake at the start of the experiment were comparable for all cells (not shown).

Data are presented as the mean ± SD of three independent experiments, each performed in triplicate; *$p < 0.05$, by Student's t test between the indicated conditions and the empty vector control. See also Figure S3.